THE CONTRIBUTION OF MICROSTRUCTURE TO THE FRACTURE TOUGHNESS OF HYPOEUTECTIC Al-Si CASTING ALLOY

Mahmoud F. Hafiz [1] and T. Kobayashi [2]

1. Al-Azhar University, Faculty of Engineering, Department of Mechanical Engineering,
   Nasr City, Cairo, Egypt
2. Toyohashi University of Technology, Department of Production Systems Engineering,
   Aichi 441, Japan.

Introduction

The attractions of aluminium-silicon (Al-Si) alloys for use in engineering applications are numerous. These alloys have reasonable mechanical properties, light weight and excellent castability [1]. Furthermore, silicon can form in different morphologies (e.g. plate-like and fibrous) depending on the presence or absence of certain additives, i.e. modifiers [2-6]. Thus, a wide range of mechanical properties may be achieved from a specific alloy composition.

In view of the attractive possibility of lowering the manufacturing cost through more extensive utilization of the cast components, it is envisaged that the future of cast aluminium alloys, in particular Al-Si alloys, can be further extended once a data bank of the so called the triangle relationship (i.e. the relationship among the production parameters, microstructure and mechanical behaviour) is obtained. This will satisfy the need of the design engineer and increase the confidence in the cast product. Consequently, casting alloys will be a major contender to wrought alloys, and thus many fabricated parts may be replaced by casting components.

The present investigation aims to evaluate the dynamic fracture toughness of an hypoeutectic Al-Si casting alloy produced under a variety of solidification cooling rates with different strontium levels. An attempt to clarify the interplay between the microstructure and mechanics oriented approaches is carried out. The fracture phenomena in the alloy under consideration are also investigated. In the study of fracture both microstructural and mechanics aspects are taken into consideration.

Experimental Procedures

The material used in this study is an hypoeutectic Al-Si alloy whose chemical composition (in mass%) is 8Si, 0.001Mn, <0.01Mg, 0.004Cu, 0.0008P, 0.0003Fe and balance of Al. The modified versions of the present alloy are treated by 0.017 and 0.03 mass%Sr. The molten metals are degassed using argon (Ar) gas prior to casting into either steel mould and graphite mould. Details concerning Sr addition and degassing process in addition to casting conditions are reported elsewhere [5,7].

The microstructure of the present alloy is monitored quantitatively using an image analysis system. The microstructural parameters considered here are the mean dendrite arm spacing (λ_d), the mean free path

(MFP) across the dendrites (i.e. in the interdendritic areas), the eutectic-Si characteristics {equivalent diameter (DE), aspect ratio (AR) and shape factor (SF)} and Si-particle spacing (λ_{Si}). These are compiled in Table 1. Definitions of these parameters along with schematic illustrations can be found in Ref. 7.

Table 1 The microstructural parameters considered in the present study.

Sr Content (mass%)	Mould Type	λ_d (μm)	MFP (μm)	DE (μm)	AR	SF	λ_{Si} (μm)	$(\lambda/DE)_{Si}$	Eutectic-Si Morphology
0.000	Graphite	100.51	57.54	13.10	4.10	2.58	4.80	0.34	
	Steel	84.85	47.59	4.56	3.48	2.41	3.75	0.82	
0.017	Graphite	86.45	47.02	1.23	1.50	1.44	3.75	3.04	
	Steel	65.57	34.37	0.62	1.46	1.41	2.32	3.76	
0.030	Graphite	63.87	32.98	0.79	1.40	1.38	2.89	3.65	
	Steel	53.04	26.39	0.57	1.29	1.26	2.28	3.99	

20 μm

Dynamic fracture toughness characterized by J-integral concept is evaluated using three point bend (3PB) specimen following multiple specimen method. Tests are carried out using a Charpy tester of 490J capacity.This machine is equipped with a Computer Aided Instrumented (CAI) system [8]. Using this system facilitates recording the load-deflection diagram.

For recording of the dynamic crack resistance curve (R-curve), a special experimental technique is necessary, which makes it possible to supply different energy values to the specimen. For this purpose different methods are known [8-11] but the most important is the stop block technique [8, 10]. Here different amounts of stable crack growth are produced by varying the limitation of deflection. This limitation can be accomplished by hardened steel blocks as shown in Fig. 1.
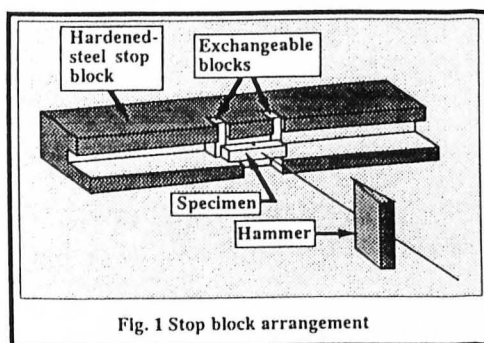

Fig. 1 Stop block arrangement

The blunting line in the R-curve is defined using the equation of Landes and Begley [12]

$$J = 2\sigma_{flow} * \Delta a$$

The dynamic flow stress (σ_{flow}) is estimated from the Py and Pm of the instrumented Charpy notched

specimen using the equation proposed by Server [13].

$$\sigma_{flow} = 0.0467 \{(Py+Pm) / 2\}$$

Results and Discussions

Effect of Sr Level and Solidification Cooling Rate

The variation of the dynamic fracture toughness (Jd) as a function of Sr level and solidification cooling rate is presented in Fig. 2. As can be seen, increasing the solidification time (graphite mould cast) is accompanied by decreasing of the Jd value. Observing the data compiled in Table 1 suggest that this loss of credits might be due to the microstructural difference as a consequence of the variation of the solidification cooling rate. At slow cooling rate, the eutectic-Si is coarser and slender (i.e. with larger DE and higher AR) and the MFP is relatively large. These features are judged to be favorable for initiating and propagating fracture at low level of energy. Thus low dynamic fracture toughness would be expected. However, independent of the casting conditions, the preponderant effect concomitant

Fig. 2 Effect of Sr content and solidification cooling rate on the dynamic fracture toughness of hypoeutectic Al-Si casting alloy.

with Sr addition, resulted in a dramatic increase in the dynamic fracture toughness. The improvement in the crack initiation resistance (Jd) agrees with the change in the mode of fracture as well as the fracture pattern reported in the present work (will be shown later). It is worthwhile noting that higher dynamic fracture toughness has been achieved when Sr modification is combined with fast cooling rate (steel mould cast). According to Hahn [14] the crack initiation in hard particle (i.e. eutectic-Si) is assisted by plastic deformation of the surrounding matrix but requires an additional stress riser such as dislocation pile-up or a defect in the particle. As a result, the coarser the particle the higher the eligibility (i.e. the probability) for producing cracks and correspondingly low dynamic fracture toughness. This explains the improvement in the fracture toughness with increasing Sr addition (fine-fibrous eutectic-Si).
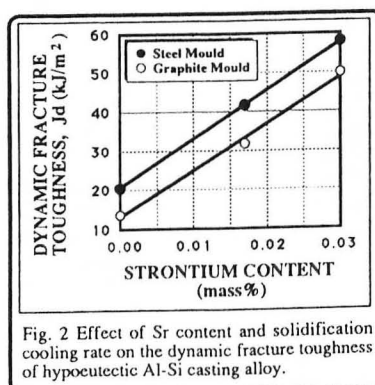
Relationship between Dynamic Fracture Toughness, Dendrite Spacing and MFP

The relationship between the dynamic fracture toughness, the dendrite spacing (λ_d) and the mean free path across the Al-rich phase (MFP) is shown in Fig.3. As can be seen in Fig. 3a, the decrease in λ_d causes an improvement in the dynamic fracture toughness. It is interesting to note that, a smaller λ_d is characteristic of fast cooled, 0.03 mass% Sr modified alloy. In other words, the decrease in λ_d is associated with a fine fibrous eutectic-Si. The fracture process of the present alloy, under dynamic loading, is dominated by the situation in the areas in the interdendritic structure (as will be shown later). Therefore, relating the change in the dynamic fracture toughness directly to the dendrite spacing seems to be naive. However, the decrease of the dendrite spacing, λ_d, is judged to play an indirect role through a more uniform distribution of eutectic mixture with finer Si-particles. This in turn improves the dynamic fracture toughness in a dramatic fashion.

In relation to the MFP as shown in Fig. 3b, a decrease in the dynamic fracture toughness with an

109

increase in MFP is apparent. One possible explanation to the deleterious effect of the increase in the MFP is as follows. Since the crack initiates at Si-particles located in the MFP (eutectic region), a large MFP will facilitate the initiated crack to propagate for a long distance in a media where Si is prevailing. This in turn results in a large loss of the load carrying capacity at an early stage of plastic deformation and thus low dynamic fracture toughness.
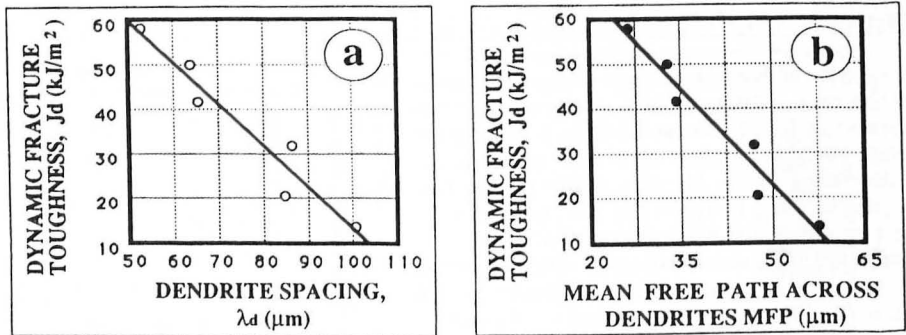

Fig. 3 Dynamic fracture toughness as a function of the dendrite spacing and the mean free path across the dendrites.

To shed more light upon the importance of the MFP, another representation of the data of Fig. 3 is given in Fig. 4. In this figure, the fracture toughness data is related to the structural integrity parameter ϕ [=MFP/λ_d]. Obviously, if the change in the dendrite spacing, λ_d, has a direct impact on the dynamic fracture toughness, one would expect an increase in the dynamic fracture toughness with an increase in the parameter ϕ (i.e. decrease of λ_d). Since this is not the trend in the data displayed in Fig.4, it can be suggested that it is the MFP that is the controlling factor. This opinion seems to be a departure from the traditional belief that the mechanical behaviour

Fig. 4 The dynamic fracture toughness of hypoeutectic Al-Si alloy as a function of the structural integrity parameter ϕ.

should be related to the dendrite spacing [15, 16]. However, good correlation between the dynamic fracture toughness presented here as well as the other mechanical properties [7,17] and the parameter ϕ has been noted. Therefore, the proposed structural integrity parameter, ϕ, is apromising factor having an influential role in controlling the mechanical properties and the deformation behaviour of hypoeutectic Al-Si alloys at certain stages in the fracture process.
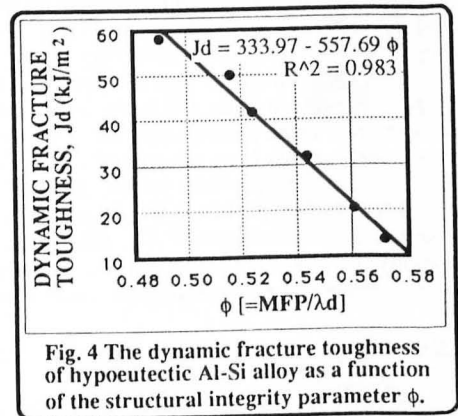
Relationship between Dynamic Fracture Toughness and Eutectic-Si Characteristics:

Figure 5 shows the dynamic fracture toughness of hypoeutectic Al-Si casting alloy as a function of DE, AR and SF of eutectic-Si-particles. As can be seen, the material with finer eutectic-Si or a rounder cross-section tolerates higher resistance for fracture initiation under dynamic fracture condition. As it has been stated in [18], the large particles may fail at a relatively low strain. The presence of such particles in a highly strained region (i.e. a crack front) is judged to cause a large premature voids.

Occurrence of such large voids limits the straining capacity of the surrounding matrix material. Consequently, low deformation energy would be spent in the plastic zone till the onset of void formation. This lowers the fracture toughness (cf. Fig. 5).

Dynamic Fracture Toughness, Eutectic-Si Spacing, and the Ratio $\lambda/DE)_{Si}$ Relationship
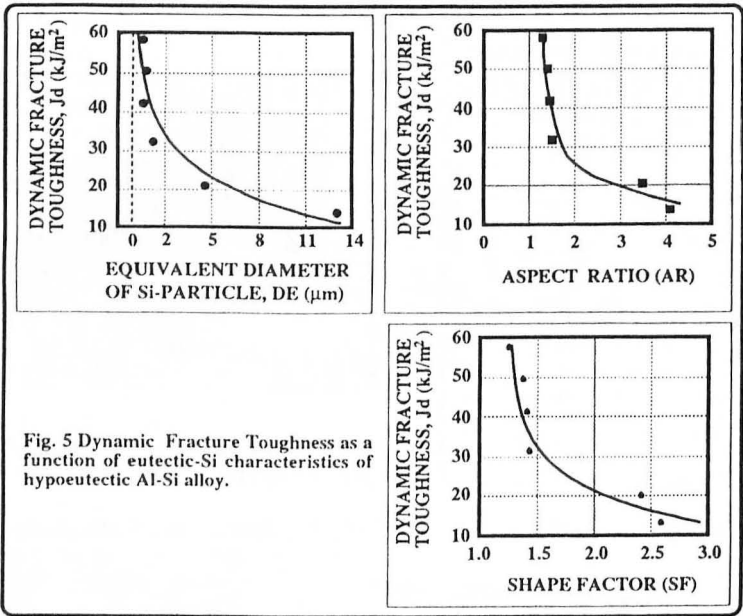

Fig. 5 Dynamic Fracture Toughness as a function of eutectic-Si characteristics of hypoeutectic Al-Si alloy.

Figure 6 shows the variation of the dynamic fracture toughness as a function of the Si-particle spacing (λ_{Si}). The dynamic fracture toughness is also presented in Fig. 6 as a function of $\lambda/DE)_{Si}$. It is obvious that an increase in the Si-particle spacing is concomitant with a loss of the dynamic fracture toughness. In contrast, dramatic improvement in the dynamic fracture toughness corresponds to an increase in the ratio $\lambda/DE)_{Si}$. It seems that the increase in the ratio $\lambda/DE)_{Si}$ has affected the stress-strain state in the matrix material between the nucleated voids. Thus the plastic work required to expand these voids, until they coalesce, is increased. This leads to the suggestion that $\lambda/DE)_{Si}$ can be considered as a mean to enhance the dynamic frac-
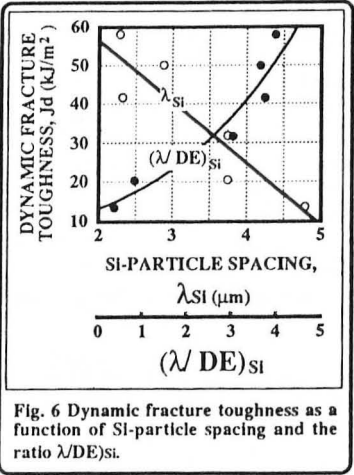

Fig. 6 Dynamic fracture toughness as a function of Si-particle spacing and the ratio $\lambda/DE)_{Si}$.

111

ture toughness of hypoeutectic Al-Si casting alloy.

Since the dynamic fracture toughness is expected to depend on the amount of work done required for void growth, it is relevant to relate the dynamic fracture toughness to the void growth parameter, VGP$(=\sigma_y*\lambda/DE)_{Si}$ where σ_y is the yield stress of the material) proposed by the authors [19]. This is shown in Fig. 7. It is worthwhile noting that the dynamic fracture toughness fits well on a line of positive slope reflecting the improvement in Jd with an increase in VGP. Comparing this result with the previous published data concerning the static fracture toughness of the same alloy [19] suggests that VGP is not an overriding factor in controlling the fracture toughness of the present alloy.
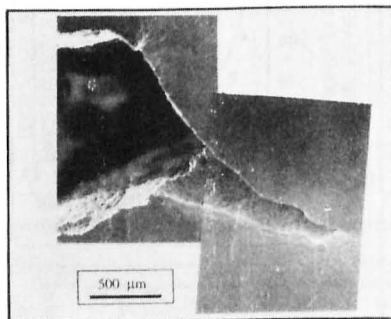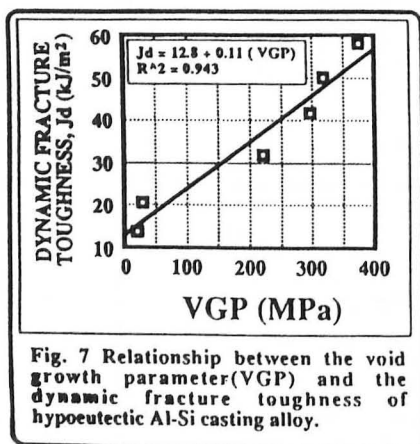

Fig. 7 Relationship between the void growth parameter(VGP) and the dynamic fracture toughness of hypoeutectic Al-Si casting alloy.

Fig. 8 Fracture path as observed on the external surface of nonmodified alloy using SE?M (steel mould cast).

Fracture Characteristics under Dynamic Fracture Toughness Test Conditions.

(i) Observations on external surface: Figure 8 illustrates the fracture process that occurs during the dynamic fracture toughness test, as detected on the external surface of a nonmodified alloy using a scanning electron microscope. Plastic blunting at the main crack tip (i.e. fatigue precrack) is likely to occur before the crack propagates through the plastic zone. The initial fracture of the eutectic-Si and the strain concentration in the surrounding matrix can be observed well ahead of the propagating crack. The localized plasticity is depicted at a high magnification in Fig. 9. On further loading some of the plastically deformed regions would be expected to undergo rupture causing the microcracks to link up with each other and/or with the main crack front.

Regarding the modified version of the present alloy, the micrograph of Fig. 10 show that the fracture process is closely similar to that of the nonmodified one. In other words, the microstructural variation concomitant with Sr modification does not strongly.

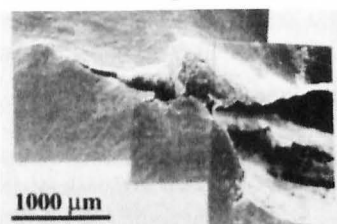Fig. 9 Localized plasticity observed ahead of the crack tip.

Fig. 10 The fracture mechanics in an alloy modified with 0.03 mass%Sr (steel mould cast).

influence the sequence of crack initiation and propagation processes just described.

(ii) Examination of the mid-plane section: Figure 11a shows an optical micrograph for a mid-plane section of nonmodified alloy. This micrograph indicates that progressive damage process takes place in a relatively extended zone ahead of the crack.. It is worthwhile noting that the individual cracked Si-particles join together giving rise to microcracks. These micro-cracks are likely to coalesce together then growing to form a lateral crack, or to join with the main crack. Another merit is that the crack moves through the interdendritic areas avoiding the Al-dendrites.

Examination of the mid-section of the modified alloys confirmed the fact that the fundamentals of the fracture process are the same as those found for the nonmodified alloy. However, it is of interest noting that the crack changed its habit and propagates through the Al-dendrite in a transgranular fashion when it is possible. This is shown clearly in Fig. 11b. This explains the improvement in the dynamic fracture toughness.

(iii) Fracture surface observations
The fracture pattern of the nonmodified hypoeutectic alloy as revealed by SEM is shown in Fig. 12. A complex pattern reflecting a low energy is delineated in this figure. Cloven Si-particles can be seen as the major area on the fracture surface (Fig. 12a). These are also shown in Fig. 12b at high magnification. The features of Fig. 12 agree with the low fracture toughness displayed by the present alloy in the nonmodified state under dynamic fracture toughness test conditions..

The general features of the fracture surface of the 0.03 mass% Sr modified alloy (steel mould cast) is shown in Fig. 13a . The main features in this fractograph are a majority of dimple colonies surrounded by a smooth rippled pattern. These are shown at high magnification in Fig. 13b. The features depicted in Fig. 13 are considered to be typical features of a ductile fracture. This dramatic change in the fracture pattern can be attributed to the apparent change in the eutectic region referred to in Table 1. The features delineated in this figure explain the significant improvement in the dynamic
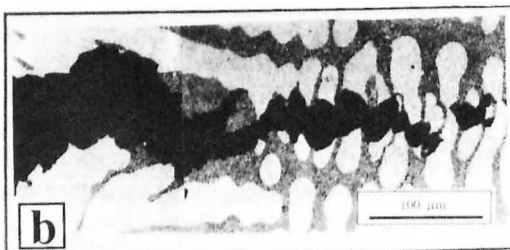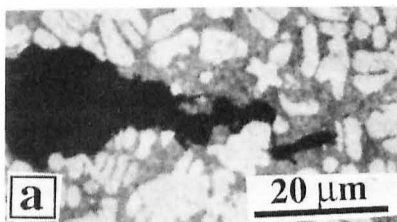

Fig. 11 Fracture path detected in the mid-section (a) nonmodified alloy and (b) modified with 0.03 mass%Sr (steel mould cast).
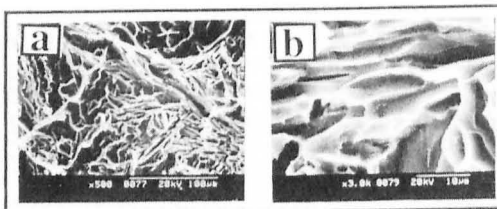

Fig. 12 The features of the fracture surface of nonmodified alloy (steel mould cast).
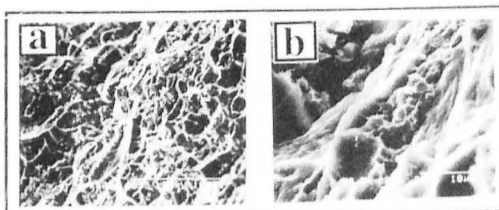

Fig. 13 The fracture pattern in an alloy modified with 0.03 mass%Sr (steel mould cast).

113

fracture toughness and reflect the influential role of the Si-particle (size and morphology) in the fracture process.

Conclusions

1. Since the crack is almost always initiates by fracturing of the Si-particles and prefers to propagate into the eutectic areas located in the mean free path (MFP) across the dendrites (i.e. in the interdendritic structure), it is largely believed that the dynamic fracture toughness is directly affected by MFP rather than the dendrite spacing (λ_d). However, dynamic fracture toughness is found to correlate well with the structural integrity parameter, ϕ {=MFP/λ_d}, proposed by the authors.

2. Fine eutectic-Si particles with low aspect ratio and rounder cross-section result in a significant improvement in the dynamic fracture toughness of the present alloy owing to their influence on the void nucleation resistance as well as the local strain concentration as affected by the void size.

3. Decreasing the eutectic-Si spacing in combination with increasing the value of λ/DE)$_{Si}$ has influenced the dynamic fracture toughness of the alloy under consideration, significantly. The former causes a gradual loss of the load bearing capacity after void nucleation while the latter reduces the interaction stress field around the Si-particles, so that the level of plastic deformation in the neighborhood of these particles is reduced. This in turn affects the void nucleation and the subsequent void growth aspect of fracture.

4. The good correlation found between the void growth parameter, VGP {=σ_y * λ/DE)$_{Si}$} and the dynamic fracture toughness emphasizes that Hahn and Rosenfield's equation [20] should include the term λ/DE of the particle rather than the interparticle spacing, λ.

References

1. L.F. Mondolfo, Aluminium Alloys;Structure and Properties (Butterworths, London,1976).
2. A. Hellawell, Progress in Mater. Sci., Vol. 15 (Pergamon Press, 1973), 3.
3. M.M. Haque, Met. Forum, 6 (1983), 54
4. M.D. Hanna, Shu-Zu-Lu and A. Hellawell, Metall. Trans. 15A (1984), 459.
5. M.F. Hafiz and T. Kobayashi, Trans. J. Foundrymen's Soci, 12 (1993) 115.
6. M.F. Hafiz and T. Kobayashi, J. Inst. Light Metals, 44 (1) (1994), 28.
7. M.F. Hafiz and T. Kobayashi, Cast Metals J. (To be published).
8. T. Kobayashi , I. Yamamoto and M. Niinomi., J. Testing and Evaluation, 21 (3) (1993), 145.
9. T. Kobayashi, Int. J. of Fracture, 23 (1983), 105.
10. H.A. Crostack, H.D.Steffens and A.H. Engelhardt, Analytical and Experimental Fracture Mechanics, ed. G.C. Sih and M. Mirabile, (Sijthoff and Noordnoff (1981), 507.
11. T. Kobayashi, Engineering Fracture Mechanics, 1 (19) (1984), 49.
12. J.D. Landes and J.A. Begley, Fracture analysis, (ASTM-STP 560) (1974), 170.
13. W.L. Server, ASTM-STP 668 (1979), 493.
14. G.T. Hahn, Metall. Trans. 15A (1984), 947.
15. R.E. Spear and G.R. Gardner, AFS Trans. 71 (1963), 209.
16. K.J. Oswalt and M.S. Misra, AFS Trans., 88 (1980), 845.
17. M.F. Hafiz, Ph.D. thesis, Toyohashi University of Technology, Japan (1994).
18. A. Saigal and J.T. Berry, AFS Trans., 93 (1985), 699.
19. M.F. Hafiz and T. Kobayashi, Scripta Metall. et Mater. 30 (4) (1994), 475.
20. G.T. Hahn and A.R. Rosenfield, Metall. Trans. 6A (1975), 653.